



Title	Ultralong C(sp ³)-C(sp ³) Single Bonds Shortened and Stabilized by London Dispersion
Author(s)	Shimajiri, Takuya; Kawakami, Yuta; Kawaguchi, Soki; Hayashi, Yuki; Hada, Kazuto; Suzuki, Takanori; Ishigaki, Yusuke
Citation	Synlett, 34(10), 1147-1152 https://doi.org/10.1055/a-1934-1346
Issue Date	2022
Doc URL	http://hdl.handle.net/2115/90607
Type	article (author version)
File Information	Synlett 2022. Cluster_Dispersion Effects.pdf



[Instructions for use](#)

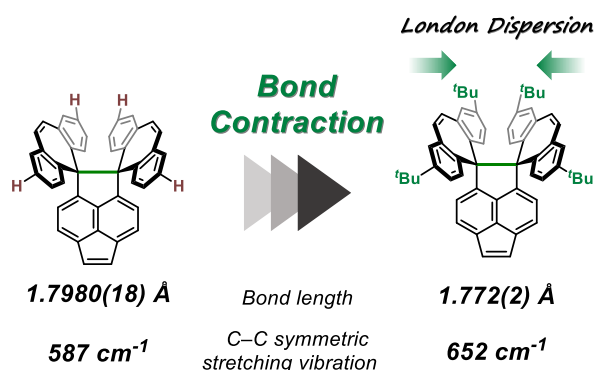
Ultralong Csp^3-Csp^3 Single Bonds Shortened and Stabilized by London Dispersion

Takuya Shimajiri*^{a,b}
 Yuta Kawakami^a
 Soki Kawaguchi^a
 Yuki Hayashi^a
 Kazuto Hada^a
 Takanori Suzuki^a
 Yusuke Ishigaki*^a

^a Department of Chemistry, Faculty of Science, Hokkaido University, Sapporo, Hokkaido 060-0810, Japan.

^b Creative Research Institution, Hokkaido University, Sapporo, Hokkaido 001-0021, Japan.

t.shimajiri@sci.hokudai.ac.jp, yishigaki@sci.hokudai.ac.jp



Received:
 Accepted:
 Published online:
 DOI:

Abstract A carbon-carbon (C–C) single bond longer than 1.7 Å shows unique bond flexibility, even though a C–C single bond is typically rigid and robust. We report here that the bond length of a flexible C–C single bond surrounded by bulky alkyl groups on novel hexaphenylethane-type hydrocarbons could be affected by even weak non-covalent interactions such as London dispersion. Thanks to London dispersion, an ultralong and flexible C–C single bond exhibits an obvious bond contraction. X-ray analyses and Raman spectroscopy provide direct information regarding the bond length and strength, and density functional theory calculations explain the bond contraction driven by London dispersion. An extremely elongated C–C bond with flexibility would be a good probe for quantifying even weak interaction, which is usually difficult to detect, as a change in bond length.

Key words strained molecules, hydrocarbons, long C-C bonds, X-ray analysis, London dispersion

Introduction

Covalent bonds are the strongest form of chemical bonding, and connect atoms to create a molecular skeleton as a primary structure. Non-covalent interactions are weaker than covalent bonds, but are important for determining molecular geometries^{1,2} and chemical reactivities.³ Among non-covalent interactions, the London dispersion (LD) interaction is quite weak and is often considered to be negligible compared to other interactions such as electrostatic interaction and hydrogen bonding.⁴ On the other hand, it has recently been found that LD force stabilizes intrinsically unstable compounds^{5–7} and geometries,⁸ thus significantly impacting the selectivity of chemical reactions.^{9–12}

For example, hexaphenylethane derivatives (HPEs) are representative compounds with a long Csp^3-Csp^3 single bond, which can be stabilized by LD force. Non-substituted HPE **I** was first proposed by Gomberg in 1900, but the parent HPE **I**, if formed, undergoes Csp^3-Csp^3 bond fission into two triphenylmethyl radicals to isomerize thermodynamically more stable α,p -dimer **II** (Figure 1).^{13–15} The introduction of bulky *tert*-

butyl groups at all of the *meta* positions on the phenyl groups of the parent HPE **I** makes it possible to isolate an σ -bonded molecule **III** as a stable entity, and its formation was confirmed by X-ray analysis.^{5,16} The X-ray structure of HPE **III** clearly shows an unusually long Csp^3-Csp^3 bond [1.67(3) Å at 175 K]; its standard length is 1.54 Å. This is because *tert*-butyl groups can function not only as protecting groups to prevent the formation of the corresponding α,p -dimer but also as dispersion energy donors (DEDs) to stabilize the α,α -bonding structure **III**, which was theoretically explained by Grimme and Schreiner *et al.*^{17–19} Also, Schreiner *et al.* prepared the remarkably stable diamondoid dimer **IV** with a decomposition temperature at 220 °C thanks to the LD interaction between two diamondoids, despite its very long Csp^3-Csp^3 single bond with a bond length beyond 1.7 Å.^{6,20}

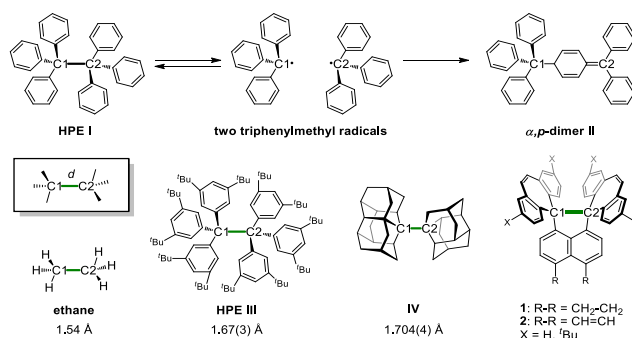


Figure 1 Examples of an unusual Csp^3-Csp^3 distance between C1 and C2 atoms.

Recently, we reported that HPE-type hydrocarbons **1,2-H** with two spiro-dibenzocycloheptatriene (DBCHT) units have an extremely elongated Csp^3-Csp^3 single bond with a bond length of around 1.8 Å.²¹ Among them, **2-H** showed a Csp^3-Csp^3 bond length of 1.806(2) Å at 400 K, which was determined experimentally by X-ray analysis and demonstrated by Raman spectroscopy. In addition, we discovered that such an extremely elongated Csp^3-Csp^3 single bond endows a unique bond "flexibility", because it exhibits reversible bond expansion

and contraction under the influence of external stimuli such as light and heat.²² Herein, we conceived that such a flexible bond should be affected by even very weak interactions that are usually considered negligible.

In this paper, we designed and synthesized novel hydrocarbons by introducing *tert*-butyl groups as DEDs into DBCHT units on **1** and **2** with a flexible bond to investigate how the dispersion forces affect the bond length, which was verified by X-ray analysis and density functional theory (DFT) calculations. As a result, we experimentally revealed that the LD interaction effectively contracts an extremely elongated flexible Csp^3-Csp^3 single bond in pyracene-type and dihydropyracylene-type HPEs (**1** and **2**).

Results and Discussion

Molecular Design

LD is a ubiquitous attractive interaction found in organic molecules. It is difficult to recognize the effect of LD because it is very weak. Therefore, bulky alkyl groups are often used as DEDs to avoid being overwhelmed by stronger interaction. On the contrary, the contiguity of large alkyl groups has repulsive effects, which could cause bond expansion.²⁰ Herein, we newly designed hydrocarbons **1-*t*Bu** and **2-*t*Bu** with a flexible Csp^3-Csp^3 single bond to investigate whether the introduction of *tert*-butyl groups induces either repulsive or attractive force, resulting in bond expansion or contraction.

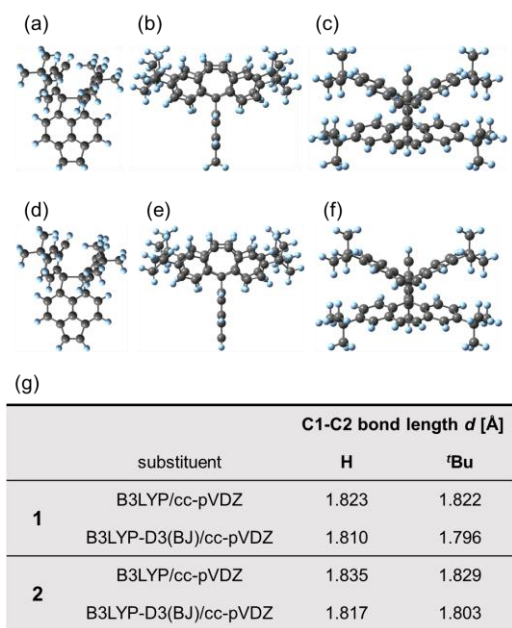


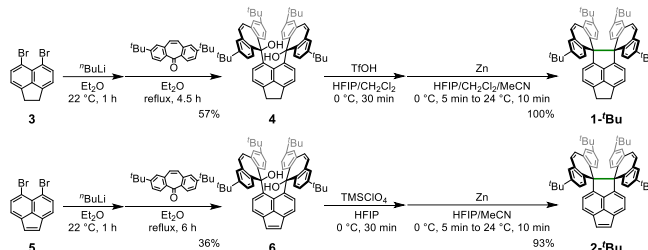
Figure 2 Optimized structures determined by DFT calculations (B3LYP-D3(BJ)/cc-pVDZ) for **1-*t*Bu** [(a) front, (b) side and (c) top views], **2-*t*Bu** [(d) front, (e) side and (f) top views]. (g) Bond length *d* of optimized structures for hydrocarbons **1** and **2**.

Initially, the substituent effects on C1-C2 bond length were investigated by DFT calculations. The optimized structures of **1,2-*t*Bu** calculated at the B3LYP/cc-pVDZ level of theory with a small amount of dispersion show almost the same C1-C2 bond length (*d*) as those of the corresponding non-*tert*-butylated derivatives **1,2-H**, which means that *tert*-butyl groups at the *para*-positions of a Csp^3 atom do not produce steric hindrance (Figure 2). By considering that B3LYP/cc-pVDZ is not suitable for evaluating the effects of DEDs, we performed optimization considering the D3(BJ) dispersion parameter of Grimme.²³ As a

result, deviation of the C1-C2 bond length with and without *tert*-butyl groups is outstanding between **1,2-*t*Bu** and **1,2-H**. Thus, it is anticipated that the LD force would be preferable for contracting the Csp^3-Csp^3 single bond.

Preparation of hydrocarbon **1-*t*Bu** and **2-*t*Bu**

A key building block, 2,8-di-*tert*-butyldibenzosuberone, was newly synthesized over 8 steps from 3-*tert*-butyl-1-bromobenzene (Scheme S1). As shown in Scheme 1, diols were obtained in respective yields of 57% and 36% by lithiation of the corresponding dibromo derivatives **3,5** followed by the reaction with 2,8-di-*tert*-butyldibenzosuberone.²⁴ Diols **4,6** were then exposed to acidic conditions in the presence of 1,1,1,3,3,3-hexafluoro-2-propanol (HFIP), and the resulting precursor dications were directly reduced with Zn powder to give desired hydrocarbons **1-*t*Bu** and **2-*t*Bu** in respective yields of 100% and 93%.²⁵ The formation of **1-*t*Bu** and **2-*t*Bu** was confirmed by (HR)-MS and ¹H NMR spectra in CDCl₃, which showed sharp signals assigned to closed-shell species in both cases.



Scheme 1 Preparation of hydrocarbons **1-*t*Bu** and **2-*t*Bu**.

In the ¹³C NMR spectra of **1,2-*t*Bu**, there is a characteristic signal assigned to the carbon atoms of the elongated C1-C2 bond in the quaternary Csp^3 region (84.88 ppm for **1-*t*Bu** and 85.88 ppm for **2-*t*Bu**). Compared to those for non-*tert*-butylated derivatives (86.30 ppm for **1-H** and 87.46 ppm for **2-H**), a slight upfield shift was observed for **1-*t*Bu** and **2-*t*Bu**. This result is consistent with the upfield shift observed in the shorter C-C single bond.^{21,22,26,27}

X-ray analysis

Recrystallization of **1-*t*Bu** and **2-*t*Bu** from hexane gave single crystals that were suitable for X-ray diffraction measurement. In the case of **2-*t*Bu**, its X-ray structure exhibits disorder, and the same site is occupied by two structures with a different flipping direction of the DBCHT units in a 65:35 ratio. The following section discusses the structural parameters for **1-*t*Bu** and the major component of **2-*t*Bu**. X-ray structures of **1-*t*Bu** and **2-*t*Bu** adopt unique unsymmetric geometries, both of which are similar to those of **1,2-H** (Figure 3). A remarkable point is contraction of the central C1-C2 single bond by as much as about 0.026 Å (1.5%). Thus, the length of 1.7980(18) Å for **2-H** decreases to 1.772(2) Å for **2-*t*Bu**. This holds true for another comparison; from 1.773(3) Å for **1-H** to 1.7596(17) Å for **1-*t*Bu**, when X-ray analyses were conducted at 200 K. The distances between the central carbon atoms of the neighboring *tert*-butyl groups in different DBCHT units are 5.549(2) and 5.449(2) Å for **1-*t*Bu** and 5.273(4) and 5.534(4) Å for **2-*t*Bu**, respectively. Such proximity of the *tert*-butyl groups is not enough to cause steric repulsion, but is enough to gain stabilization by the LD force (Figure S21),^{8,28} and thus the observed contraction most likely is due to the LD force. DEDs would have less of an effect at higher temperature. When we conducted X-ray measurements at 400 K, the *d* value for **1-*t*Bu** marginally increased upon heating, but was still smaller than that

for **1-H** at the same temperature. In this way, LD force is working even at high temperature to shorten and to strengthen the elongated bond. The nature of such an elongated Csp^3-Csp^3 single bond was theoretically studied by quantum theory of atom in molecules (QTAIM)²⁹ and natural bond orbital (NBO) analyses (Figure S22,S23).

The non-covalent interaction (NCI) plots³⁰ of **1-*t*Bu** and **2-*t*Bu** at the B3LYP/6-311+G** level of theory using the X-ray coordinates measured at 200 K as an initial structure show that *tert*-butyl groups on the DBCHT units exert not repulsive, but rather attractive effects due to the LD force.

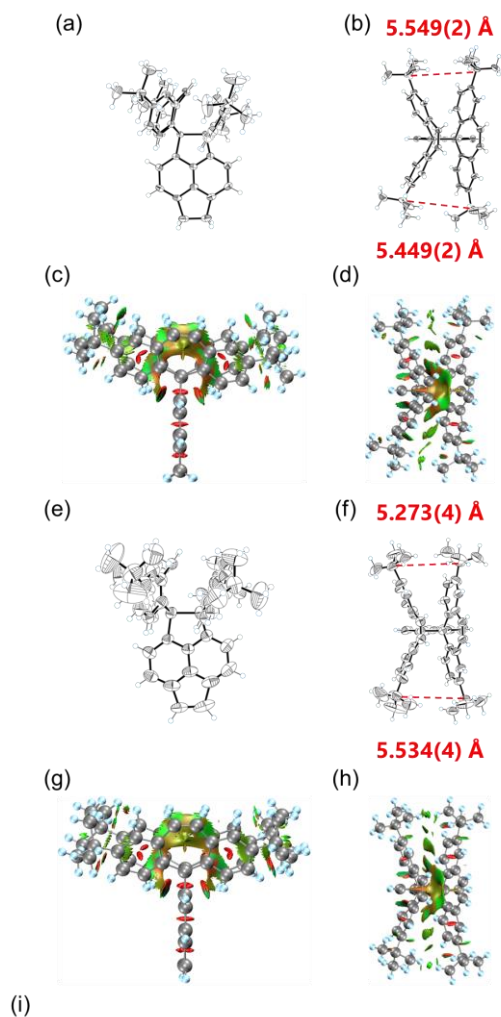


Figure 3 ORTEP drawings at 200 K for **1-*t*Bu** [(a) front and (b) top views] and **2-*t*Bu** [(e) front and (f) top views]. X-ray structures of **2-*t*Bu** exhibit disorder, and the same site is occupied by two structures with a different flipping direction of the DBCHT units in a 65:35 ratio. The minor component of **2-*t*Bu** is omitted for clarity. (i) Central C–C bond lengths at each temperature. NCI plots (isovalue= 0.5 a.u.) for **1-*t*Bu** [(c) side and (d) top views] and **2-*t*Bu** [(g) side and (h) top views] obtained at the B3LYP-D3(BJ)/6-311+G** level of theory. Color online: blue represents strong attractive interactions, green indicates van der Waals interactions and red indicates repulsive/steric interactions.

Raman spectroscopy

Next, the stretching vibration of the elongated C1–C2 single bond was investigated by Raman spectroscopy with single crystals of **1-*t*Bu** and **2-*t*Bu** at 298 K, which gives direct information regarding the strength of the bond. The experimentally obtained and simulated Raman spectra for these hydrocarbons are shown in Figure 4. As a result, the simulated spectra by DFT calculations at B3LYP/6-31G* with a scaling factor³¹ of 0.9613 to consider anharmonicity very nicely reproduced the experimental results. The observed Raman shifts at 654 cm⁻¹ for **1-*t*Bu** and 652 cm⁻¹ for **2-*t*Bu**, which appear at a much lower energy region compared with that (993 cm⁻¹) for ethane,³² are attributed to symmetric C1–C2 stretching vibration. More importantly, the Raman shifts for **1,2-*t*Bu** are larger than those for **1-H** (582 cm⁻¹) and **2-H** (587 cm⁻¹), which are consistent with the shorter bond length in *tert*-butylated derivatives. The estimated force constant (117.9 N m⁻¹) obtained as a second derivative of the energy to the bond length by DFT calculations (M06-2X/6-31G*) for **2-*t*Bu** is 8% larger as that for **2-H** (108.3 N m⁻¹) (Figure S28).

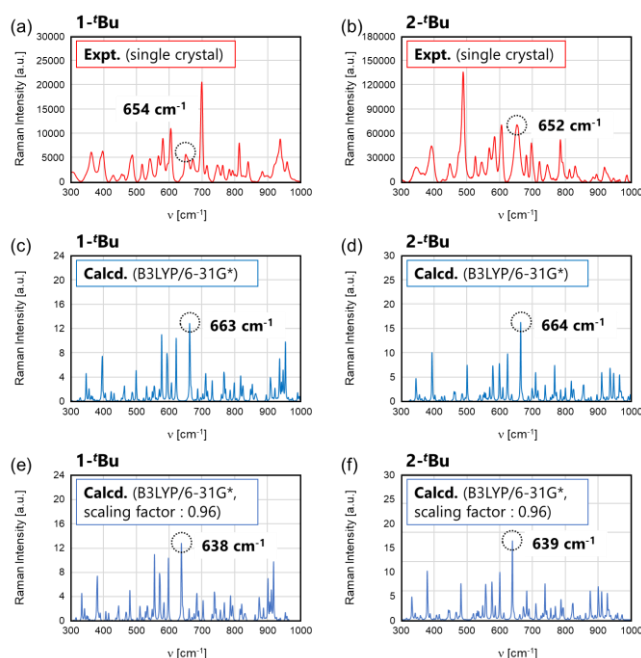


Figure 4 Raman spectra (red) measured by using a single crystal for (a) **1-*t*Bu** and (b) **2-*t*Bu** at 298 K. Simulated spectra predicted by DFT calculations at the B3LYP/6-31G* level without scaling (light blue) for (c) **1-*t*Bu** and (d) **2-*t*Bu**, at the B3LYP/6-31G* level under scaling (blue) for (e) **1-*t*Bu** and (f) **2-*t*Bu**.

Theoretical Studies for Dispersion Effect

To obtain theoretical insight into the dispersion effects, we carried out DFT calculations at the B3LYP level using the cc-pVDZ basis set. We estimated the stabilization energy by comparison of the DFT and DFT-D3(BJ) energies with the atomic coordinates obtained by X-ray structures at 200 K by computing the energy difference $\Delta E_{\text{disp}} = H_0(\text{B3LYP-D3(BJ)}) - H_0(\text{B3LYP})$. The values of ΔE_{disp} are -218 kcal mol⁻¹ for **1-*t*Bu** and -217 kcal mol⁻¹ for **2-*t*Bu**, respectively, which are much higher than those for **1-H** (-147 kcal mol⁻¹) and **2-H** (-144 kcal mol⁻¹) without *tert*-butyl group. The ΔE_{disp} correction is not exactly equal to the dispersion stabilization as the correction depends on the repulsiveness of the functional employed, but it provides an excellent estimate of the magnitude of such interaction. Therefore, the LD force affects

the stabilization of the long-bonded species accompanied by bond contraction of the ultralong and flexible Csp^3-Csp^3 bond.

Conclusion

We designed and synthesized novel hydrocarbons **1-tBu** and **2-tBu** with bulky *tert*-butyl groups potentially showing both steric hindrance and DED. The NMR measurements of **1,2-tBu** show sharp signals assigned to closed-shell long-bonded species without the formation of radical species. A long Csp^3-Csp^3 single bond around 1.76-1.77 Å was observed by X-ray analyses of **1,2-tBu**. The values of the central Csp^3-Csp^3 bond length for **1,2-tBu** are certainly smaller than those for the corresponding parent hydrocarbons **1,2-H**, even though **1,2-tBu** has sterically large alkyl moieties. Because of the shorter bond, slightly large Raman shifts corresponding to the C-C stretching vibration for **1,2-tBu** were observed, compared to those for **1,2-H**. Furthermore, theoretical examinations showed that the bond contraction is due to the LD force between bulky *tert*-butyl groups.

With the use of an extremely elongated flexible C-C bond, even weak interactions such as LD force, that are normally difficult to detect, could be visualized and quantified as a change in bond length.

Funding Information

We thank Grant-in-Aid from MEXT and JSPS (Nos. 20H02719 and 20K21184 to TSu, and 21H01912 and 21H05468 to YI) Japan. This work was also supported by the Research Program of "Five-star Alliance" in "NJC Mater. & Dev." MEXT and Masason Foundation (SK).

Acknowledgment

Click here to insert acknowledgment text. Funding sources and grant numbers should be given above in the Funding Information section.

Supporting Information

YES (this text will be updated with links prior to publication)

Primary Data

Is there **Primary Data** associated with this article? Click here to enter the Zenodo.org DOI, or click the arrow and choose NO.

Conflict of Interest

The authors declare no conflict of interest.

References and Notes

- Fenniri, H.; Mathivanan, P.; Vidale, K. L.; Sherman, D. M.; Hallenga, K.; Wood, K. V.; Stowell, J. G. *J. Am. Chem. Soc.* **2001**, *123*, 3854.
- Panigrahi, S. K.; Desiraju, G. R. *Proteins Struct. Funct. Bioinforma.* **2007**, *67*, 128.
- Jain, P.; Antilla, J. C. *J. Am. Chem. Soc.* **2010**, *132*, 11884.
- Hunter, C. A. *Angew. Chem. Int. Ed.* **2004**, *43*, 5310.
- Kahr, B.; Van Engen, D.; Mislow, K. *J. Am. Chem. Soc.* **1986**, *108*, 8305.
- Schreiner, P. R.; Chernish, L. V.; Gunchenko, P. A.; Tikhonchuk, E. Y.; Hausmann, H.; Serafin, M.; Schlecht, S.; Dahl, J. E. P.; Carlson, R. M. K.; Fokin, A. A. *Nature* **2011**, *477*, 308.
- Rösel, S.; Becker, J.; Allen, W. D.; Schreiner, P. R. *J. Am. Chem. Soc.* **2018**, *140*, 14421.
- Schumann, J. M.; Wagner, J. P.; Eckhardt, A. K.; Quanz, H.; Schreiner, P. R. *J. Am. Chem. Soc.* **2021**, *143*, 41.
- Aikawa, H.; Takahira, Y.; Yamaguchi, M. *Chem. Commun.* **2011**, *47*, 1479.
- Yamaguchi, M.; Shigeno, M.; Saito, N.; Yamamoto, K. *Chem. Rec.* **2014**, *14*, 15.
- Ikawa, T.; Yamamoto, Y.; Heguri, A.; Fukumoto, Y.; Murakami, T.; Takagi, A.; Masuda, Y.; Yahata, K.; Aoyama, H.; Shigeta, Y.; Tokiwa, H.; Akai, S. *J. Am. Chem. Soc.* **2021**, *143*, 10853.
- Eschmann, C.; Song, L.; Schreiner, P. R. *Angew. Chem. Int. Ed.* **2021**, *60*, 4823.
- Gomberg, M. *Berichte der Dtsch. Chem. Gesellschaft* **1900**, *33*, 3150.
- Gomberg, M. *J. Am. Chem. Soc.* **1900**, *22*, 757.
- Lankamp, H.; Nauta, W. T.; MacLean, C. *Tetrahedron Lett.* **1968**, *9*, 249.
- Stein, M.; Winter, W.; Rieker, A. *Angew. Chem. Int. Ed. Engl.* **1978**, *17*, 692.
- Grimme, S.; Schreiner, P. R. *Angew. Chem. Int. Ed.* **2011**, *50*, 12639.
- Rösel, S.; Balestrieri, C.; Schreiner, P. R. *Chem. Sci.* **2016**, *8*, 405.
- Rösel, S.; Schreiner, P. R. *Isr. J. Chem.* **2022**, *62*, [DOI 10.1002/ijch.202200002.] *in press*
- Fokin, A. A.; Chernish, L. V.; Gunchenko, P. A.; Tikhonchuk, E. Y.; Hausmann, H.; Serafin, M.; Dahl, J. E. P.; Carlson, R. M. K.; Schreiner, P. R. *J. Am. Chem. Soc.* **2012**, *134*, 13641.
- Ishigaki, Y.; Shimajiri, T.; Takeda, T.; Katoono, R.; Suzuki, T. *Chem* **2018**, *4*, 795.
- Shimajiri, T.; Suzuki, T.; Ishigaki, Y. *Angew. Chem. Int. Ed.* **2020**, *59*, 22252.
- Grimme, S.; Antony, J.; Ehrlich, S.; Krieg, H. *J. Chem. Phys.* **2010**, *132*, 154104.
- Preparation of diol 4**
To a suspension of 5,6-dibromoacenaphthene **3** (312 mg, 1.00 mmol) in dry Et₂O (20 mL) was added ⁿBuLi (1.56 M in hexane, 1.35 mL, 2.11 mmol) at 24 °C. After stirring at 24 °C for 1 h, 2,8-di-*tert*-butyldibenzosuberone (669 mg, 2.10 mmol) was added, and the mixture was heated at reflux for 4.5 h. Then, the mixture was cooled to 24 °C and diluted with water. The whole mixture was extracted with ethyl acetate three times. The combined organic layers were washed with water and brine, and dried over anhydrous Na₂SO₄. After filtration, the solvent was concentrated under reduced pressure. The crude product was purified by washing with MeOH (20 mL) three times to give **4** (451 mg) as a white solid in 57% yield; Mp: 193.3-203.1 °C (decomp.); ¹H NMR (400 MHz, CDCl₃): δ/ppm 7.88 (2H, d, *J* = 8.3 Hz), 7.84 (2H, d, *J* = 8.5 Hz), 7.68 (2H, dd, *J* = 2.0 Hz, 8.3 Hz), 7.25 (2H, dd, *J* = 2.1 Hz, 8.4 Hz), 6.97 (2H, d, *J* = 2.0 Hz), 6.72 (2H, d, *J* = 2.0 Hz), 6.69 (2H, d, *J* = 7.3 Hz), 6.58 (2H, d, *J* = 7.3 Hz), 5.63 (2H, d, *J* = 11.4 Hz), 5.55 (2H, d, *J* = 11.4 Hz), 3.29-3.12 (4H, m), 1.41 (18H, s), 1.18 (18H, s), 0.94 (2H, s); ¹³C NMR (100 MHz, CDCl₃): δ/ppm 149.16, 147.61, 147.41, 145.21, 138.27, 137.52, 136.41, 134.68, 133.90, 131.68, 131.54, 130.61, 129.33, 126.19, 125.01, 124.41, 124.30, 123.78, 121.38, 116.65, 78.56, 34.54, 34.08, 31.37, 31.34, 29.83; IR (ATR): ν/cm⁻¹ 3566, 2960, 2903, 2867, 1596, 1559, 1507, 1490, 1458, 1387, 1362, 1313, 1271, 1215, 1179, 1164, 1145, 1093, 1077, 1044, 1022, 946, 938, 891, 828, 814, 803, 783, 755, 731, 691, 677, 662, 650, 627, 549, 507, 491, 455, 428; LR-MS (FD) *m/z* (%): 793.49 (6), 792.49 (23), 791.48 (67), 790.48 (M⁺, bp), 772.46 (5), 500.24 (6); HR-MS (FD) Calcd. for C₅₈H₆₂O₂: 790.47498; Found: 790.47359.
- Preparation of diol 6**
To a solution of 5,6-dibromoacenaphthylene **5** (310 mg, 1.00 mmol) in dry Et₂O (20 mL) was added ⁿBuLi (1.57 M in hexane, 1.34 mL, 2.10 mmol) at 22 °C. After stirring at 22 °C for 1 h, 2,8-di-*tert*-butyldibenzosuberone (668 mg, 2.10 mmol) was added to the resulting suspension, and the mixture was heated at reflux for 6 h. The reaction mixture was allowed to cool to 24 °C, and then diluted with water, and extracted with CHCl₃ three times. The combined organic layers were washed with water and brine, and dried over anhydrous Na₂SO₄. After filtration, the solvent was concentrated under reduced pressure. The crude product was purified by column chromatography on silica gel (CH₂Cl₂/hexane =

1/3, Rf = 0.42) to give **6** (283 mg, 36%) as a pale-orange solid.; Mp: 229.5-261.3 °C (decomp.); ¹H NMR (400 MHz, CDCl₃) δ 7.86 (2H, d, J = 8.4 Hz), 7.82 (2H, d, J = 8.4 Hz), 7.69 (2H, dd, J = 2.2, 8.4 Hz), 7.27 (2H, dd, J = 2.2, 8.6 Hz) 7.00 (2H, d, J = 1.6 Hz), 6.98 (2H, d, J = 7.2 Hz), 6.75 (2H, d, J = 2.0 Hz), 6.70 (2H, s), 6.62 (2H, d, J = 7.2 Hz), 5.68 (2H, d, J = 11.2 Hz), 5.64 (2H, d, J = 11.6 Hz), 1.42 (18H, s), 1.18 (18H, s), 0.97 (2H, s) ppm; ¹³C NMR (100 MHz, CDCl₃) δ 149.50, 147.73, 147.10, 143.23, 138.93, 137.44, 134.41, 134.05, 131.70, 131.03, 130.54, 129.81, 128.70, 127.98, 125.97, 125.07, 124.52, 124.47, 123.80, 121.54, 121.11, 78.62, 34.58, 34.12, 31.35, 31.32 ppm; IR (ATR): ν/cm⁻¹ 3560, 2956, 2866, 2362, 1602, 1559, 1507, 1490, 1384, 1361, 1313, 1264, 1206, 1093, 1045, 888, 825, 805, 741, 715, 691, 668, 651, 624, 555, 506 cm⁻¹; LR-MS (FD) m/z (%): 791.44 (6), 790.44 (25), 789.44 (M⁺, 65), 788.43 (bp), 773.88 (5), 772.87 (9), 772.43 (10), 771.43 (30), 770.42 (45), 499.24 (8), 498.24 (21), 356.14 (16), 301.09 (7), 300.08 (25), 152.05 (5); HR-MS (FD): [M⁺] calcd. for C₅₈H₆₀O₂, 788.45933; found, 788.46151.

(25) **Preparation of 1⁻Bu**

To a suspension of **4** (100 mg, 126 μmol) in dry CH₂Cl₂ (1 mL) and HFIP (1 mL) was added TfOH (110 μL, 1.24 mmol) at 0 °C. The solution was stirred at 0 °C for 30 min, and added dry MeCN (2 mL) and activated Zn powder (1.24 g, 18.8 mmol) at 0 °C. After stirring at 0 °C for 5 min, the mixture was warmed to 24 °C and stirred at 24 °C for 10 min. Then, the mixture was diluted with water at 0 °C, and extracted with CH₂Cl₂ three times. The combined organic layer was washed with water, saturated NaHCO₃ aqueous solution and brine, and dried over anhydrous MgSO₄. After filtration through silica pad, the solvent was concentrated under reduced pressure to give **1⁻Bu** (95.4 mg) as a white solid in 100% yield.; Mp: 266.4-279.8 °C (decomp.); ¹H NMR (400 MHz, CDCl₃): δ/ppm 7.42 (2H, d, J = 6.9 Hz), 7.15 (2H, d, J = 7.0 Hz), 6.77 (4H, d, J = 2.1 Hz), 6.46 (4H, dd, J = 2.2 Hz, 8.7 Hz), 6.33 (4H, s), 6.23 (4H, d, J = 8.7 Hz), 3.62 (4H, s), 1.12 (36H, s); ¹³C NMR (100 MHz, CDCl₃): δ/ppm 148.10, 147.37, 141.98, 138.42, 137.81, 137.58, 135.75, 133.49, 132.46, 127.47, 127.38, 123.05, 121.26, 84.88, 33.73, 31.95, 31.21; IR (ATR): ν/cm⁻¹ 3028, 2951, 2864, 1603, 1559, 1500, 1476, 1458, 1440, 1429, 1382, 1359, 1290, 1264, 1230, 1206, 1147, 1065, 1023, 948, 902, 886, 841, 804, 792, 765, 752, 719, 703, 689, 654, 600, 511, 467, 447, 434, 430, 424, 420; LR-MS (FD) m/z (%): 759.40 (8), 758.39 (25), 757.39 (66), 756.38 (M⁺, bp); HR-MS (FD) Calcd. for C₅₈H₆₀: 756.46950; Found: 756.47015.

Preparation of 2⁻Bu

To a suspension of **6** (99.7 mg, 126 μmol) in HFIP (3 mL) was added TMSClO₄ (0.79 M in dry toluene, 1.05 mL, 830 μmol) at 0 °C. The solution was stirred at 0 °C for 30 min, and added dry MeCN (7 mL) and activated Zn powder (1.24 g, 190 mmol). After stirring at 0 °C for 5 min, the mixture was warmed to 22 °C and stirred at 22 °C for 5 min. Then, the mixture was diluted with water at 0 °C, and extracted with ethyl acetate three times. The combined organic layers were washed with water, saturated NaHCO₃ aqueous solution and brine, and dried over anhydrous Na₂SO₄. After filtration through silica pad, the solvent was concentrated under reduced pressure. The crude product was purified by column chromatography on silica gel (CH₂Cl₂/hexane = 1/5, Rf = 0.30) to give **2⁻Bu** (89.3 mg, 93%) as an orange solid.; Mp: 208.2-248.6 °C (decomp.); ¹H NMR (400 MHz, CDCl₃) δ 7.94 (2H, d, J = 6.8 Hz), 7.33 (2H, d, J = 7.2 Hz), 7.30 (2H, s), 6.79 (4H, d, J = 2.0 Hz), 6.44 (4H, dd, J = 2.4, 8.8 Hz), 6.36 (4H, s), 6.12 (4H, d, J = 8.8 Hz), 1.12 (36H, s) ppm; ¹³C NMR (100 MHz, CDCl₃) δ 153.62, 148.34, 138.16, 135.99, 135.66, 133.38, 132.45, 129.23, 127.47, 127.26, 126.91, 123.15, 85.85, 33.72, 31.13 ppm; IR (ATR): ν/cm⁻¹ 3031, 2952, 2865, 2361, 1734, 1700, 1684, 1653, 1603, 1559, 1506, 1458, 1419, 1382, 1360, 1290, 1264, 1206, 1148, 1078, 949, 908, 887, 841, 832, 802, 793, 736, 684, 668, 652, 502 cm⁻¹; LR-MS (FD) m/z (%): 757.44 (8), 756.44 (25), 755.44 (M⁺, 67), 754.43 (bp); HR-MS (FD): [M⁺] calcd. for C₅₈H₅₈, 754.45385; found, 754.45572.

(26) Takeda, T.; Uchimura, Y.; Kawai, H.; Katoono, R.; Fujiwara, K.; Suzuki, T. *Chem. Lett.* **2013**, *42*, 954.

(27) Suzuki, T.; Uchimura, Y.; Nagasawa, F.; Takeda, T.; Kawai, H.; Katoono, R.; Fujiwara, K.; Murakoshi, K.; Fukushima, T.; Nagaki, A.; Yoshida, J. *Chem. Lett.* **2014**, *43*, 86.

(28) Hwang, J.; Li, P.; Smith, M. D.; Shimizu, K. D. *Angew. Chem. Int. Ed.* **2016**, *55*, 8086.

(29) Bader, R. F. W. *Acc. Chem. Res.* **1985**, *18*, 9.

(30) Contreras-García, J.; Johnson, E. R.; Keinan, S.; Chaudret, R.; Piquemal, J. P.; Beratan, D. N.; Yang, W. J. *Chem. Theory Comput.* **2011**, *7*, 625.

(31) Wong, M. W. *Chem. Phys. Lett.* **1996**, *256*, 391.

(32) Van Helvoort, K.; Knippers, W.; Fantoni, R.; Stolte, S. *Chem. Phys.* **1987**, *111*, 445.